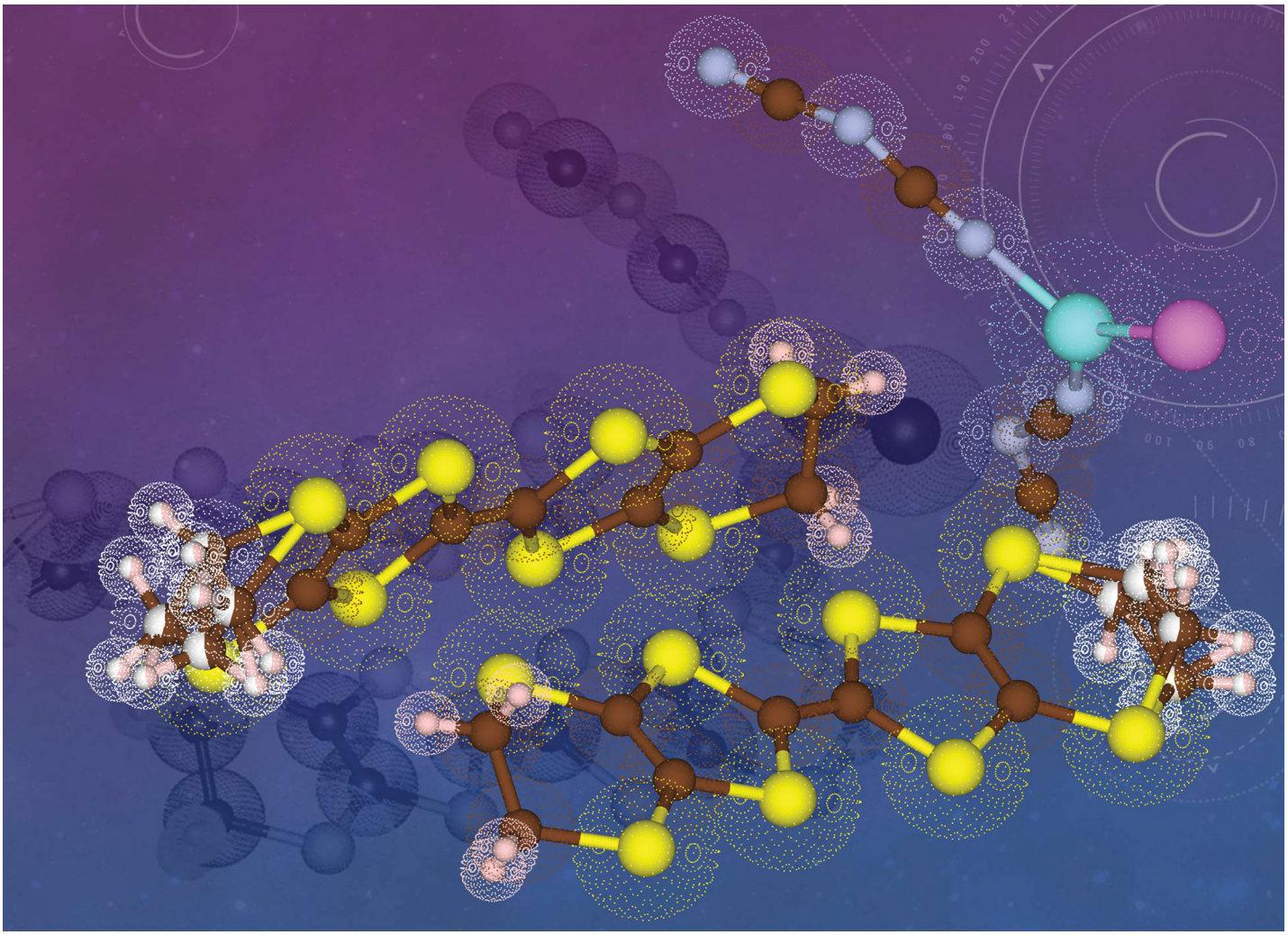

Showcasing research from Professor Naito's laboratory, Graduate School of Science and Engineering, Ehime University, Matsuyama, Japan.

Organic charge transfer complex at the boundary between superconductors and insulators: critical role of a marginal part of the conduction pathways

An organic compound has been controversially reported as two extremes for 30 years: a superconductor with the highest critical temperature among organics and an insulator. The intrinsic conduction mechanism is important for revealing the possibly universal superconducting mechanism for developing superconductors exhibiting even higher critical temperatures. The study has revealed that the conduction properties are affected by slight differences in a part of molecules, which is not involved in the conduction pathways. The important and unexpected involvement of such a marginal part of conduction pathways indicates that the rich variety of degrees of freedom should be fully considered for transforming molecular crystals to (super)conductors.

As featured in:

See Toshio Naito *et al.*, *Mater. Adv.*, 2022, **3**, 1506.

ROYAL SOCIETY OF CHEMISTRY

rsc.li/materials-advances

Registered charity number: 207890

Materials Advances

ROYAL SOCIETY OF CHEMISTRY

COMMUNICATION

View Article Online
View Journal | View Issue

Check for updates

Cite this: *Mater. Adv.*, 2022, 3, 1506

Received 8th October 2021,
Accepted 13th December 2021

DOI: 10.1039/d1ma00933h

rsc.li/materials-advances

Organic charge transfer complex at the boundary between superconductors and insulators: critical role of a marginal part of the conduction pathways†

Toshio Naito, *[abc] Hayato Takeda,[a] Yusuke Matsuzawa,[a] Megumi Kurihara,[a] Akio Yamada,[a] Yusuke Nakamura[a] and Takashi Yamamoto[abc]

κ-ET$_2$Cu[N(CN)$_2$]I (ET = bis(ethylenedithio)tetrathiafulvalene) has previously been reported as both a superconductor and an insulator. Examination of each single crystal revealed that the electrical properties are affected by slight differences in the conformation of one of the ethylene groups of ET, which is not involved in the conduction pathways.

Among the numerous existing conducting and magnetic materials, molecular crystalline materials provide a unique group of compounds with novel electronic states and peculiar physical properties. They comprise both organic and inorganic components, and often exhibit characteristics of ionic, molecular, and metallic crystals. The examples of such materials include organic charge transfer complexes (OCTCs).[1] Among the OCTCs, there is a major group of compounds sharing a characteristic molecular arrangement called κ-type (Fig. 1), where a pair ("dimer") of π-conjugated radical cations facing towards each other are arranged in such a manner that the molecular planes of adjacent dimers are nearly orthogonal to each other. The κ-type OCTCs (κ-OCTCs) are extensively studied as they exhibit various types of conducting behaviour. For example, κ-OCTCs include superconductors that exhibit T_Cs of ~10 K, which is among the highest T_Cs in organic compounds; conversely, they also include Mott insulators, which exhibit conducting properties that are completely opposite to superconductors, despite the similarities in their crystal structures.[2] The complicated relationship between the crystal structure and electrical properties in κ-OCTCs is widely observed. This relationship is a challenging problem that needs to be addressed; however, it is also the key to revealing the mechanism of superconductivity. An apparent advantage of κ-OCTCs lies in the rich variety of closely related compounds possessing well-defined crystal and band structures, allowing for a comparative study based on the systematic variation of their conducting and structural properties. Several pressure–temperature (P–T) and other related phase diagrams for κ-OCTCs have been reported, which account for the observed physical properties at the semi-quantitative level.[3] These phase diagrams are associated with those of significantly different types of superconductors, such as high-T_C cuprates, suggesting a universal mechanism of superconductivity.[4] However, a well-known exception, κ-ET$_2$Cu[N(CN)$_2$]I (**1**, Fig. 1; ET = bis(ethylenedithio)tetrathiafulvalene), was previously controversially reported to remain an insulator ($T \geq 1.1$ K and $P \leq 5.2$ kbar)[5n,u,r] as well as a superconductor ($T_C \sim 8$ K at $P > 0.1$ GPa)[5m] under identical thermodynamic conditions (1.1 to ~ 8 K at 0.1 GPa (= 1 kbar)–5.2 kbar), as no definitive differences were found between the two samples.[5] Although the electrical behaviour of single crystals of **1** is anticipated to follow the abovementioned universal phase diagrams for κ-OCTCs, the observed behaviour was substantially different from the trend in the phase diagrams, which was attributed to differences in lattice softness and are strongly influenced by short C–H···donor and C–H···anion contacts.[5u] The electrical behaviour of single crystals of **1** was reported to exhibit sample dependencies, which was related to differences in superstructures between crystals.[5j] More exactly, based on the Laue photographs and electrical resistivity measurements, the authors concluded that the qualitative differences in electrical behaviour should originate from differences in the degree of (dis)order between crystals,[5j] which is consistent with the electrical resistivity measurements under hydrostatic

[a] *Graduate School of Science and Engineering, Ehime University, Matsuyama 790-8577, Japan. E-mail: tnaito@ehime-u.ac.jp*
[b] *Geodynamics Research Center (GRC), Ehime University, Matsuyama 790-8577, Japan*
[c] *Research Unit for Development of Organic Superconductors, Ehime University, Matsuyama 790-8577, Japan*

† Electronic supplementary information (ESI) available: Electrocrystallisation conditions, single crystal X-ray structural analyses, electrical resistivity measurements, quantum chemistry calculations, band calculations (PDF). CCDC 2001301, 2001305, 2001308, 2001310–2001312, 2110351–2110354, 2110364, 2110365, 2114420–2114422, 2126205, 2126206. For ESI and crystallographic data in CIF or other electronic format see DOI: 10.1039/d1ma00933h

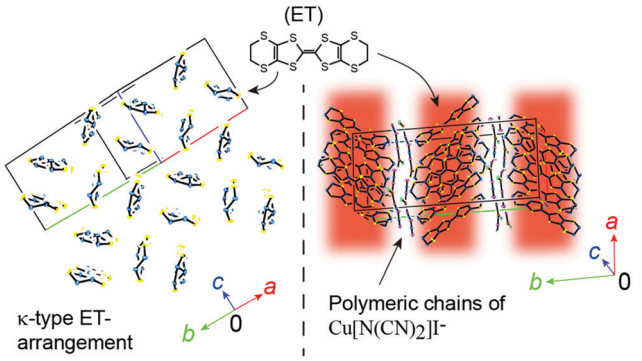

Fig. 1 Crystal structure of **1**. Blue, violet, yellow, orange, and green spheres represent C, N, S, Cu, and I atoms, respectively. The H atoms were omitted for clarity. Two-dimensional conduction pathways are highlighted in red.

pressures.[5k] Coexistence of insulating and superconducting phases, and that of two superconducting phases (T_C ~ 5 K and ~7 K) were observed by the resistivity measurements under uniaxial strain,[5g] which is consistent with uniaxial thermal expansion anisotropy observed in **1**.[5q] Apart from the inconsistency on the observed electrical behaviour, many of the previous studies suggest or indicate the importance of the ethylene group disorder in **1**[5u,v,j] to interpret the complicated and puzzling electrical behaviour of this salt.

In the present study, in addition to charge and spin degrees of freedom in the conduction pathways, and effect of superstructures on the energy band, we show that a quantitative difference in the conformation of disordered ethylene groups, located at a marginal part of the conduction pathway, also plays a crucial role in the qualitative electrical behaviour.

Pure grade chemicals were purchased and used without purification, unless otherwise noted. Single crystals of **1** were prepared by galvanostatic (2.5–5.0 μA cm^{-2}) electrolysis of a CH_2Cl_2 (Nacalai Tesque, Spectrum Grade) solution containing ET (Tokyo Chemical Industry, ground in an agate mortar immediately before use), $Na[N(CN)_2]$ (Tokyo Chemical Industry), CuI (Wako), and 18-crown-6 (Wako, dried prior to use) in a molar ratio of 1 : 4 : 4 : 6, under N_2 atmosphere at 35 °C, until black shiny platelets formed on the platinum electrode and/or at the bottom of the cell (~two weeks) (Table S1, ESI†). Large rhombus platelets were selected to confirm crystal quality and identify the lattice parameters using X-ray oscillation photographs. Crystals of good quality were cut into fragments, and those originating from the same single crystals were subjected to X-ray structural analysis (296 and 100 K) and electrical resistivity measurements (2–300 K; Quantum Design PPMS-9) in parallel, the details of which are described in the ESI.† Crystals collected from the same single crystals exhibited nearly identical electrical behaviours (Fig. S1, ESI†) and crystal structures. Meanwhile, we could not find any correlation between electrical behaviour and batches, or any correlation between the values of R and batches. Thus, we will not refer to the differences of batches in the discussion below. The cooling rates down to 100 K were generally applied to the X-ray and resistivity measurements, which were −1 and −10 K min^{-1} in the slow and fast cooling processes, respectively (Scheme S1, Fig. S5 and Table S6, ESI†).

The structure of **1** was characterized by alternating the arrangement of two-dimensional (2D) $\{(ET)_2\}^+$ and $\{Cu[N(CN)_2]I\}^-$ sheets, where only the ET sheets are responsible for conduction (Fig. 1). Every pair of ET cation radical species share an unpaired π-electron *via* overlapping HOMOs (HOMO = highest occupied molecular orbital), π-orbitals predominantly comprised sulphur 3s and 3p orbitals. The ET molecules interact to form a 2D delocalized unpaired π-electron system extended across the entire crystal (π-bands), namely 2D conduction sheets. In the unit cell of **1**, the asymmetric unit contains one general position ET molecule and the repeating unit of the polymer anion $\{Cu[N(CN)_2]I\}^-$ on a mirror plane. Our structural analysis is consistent with that of previous studies (Table S2, ESI†).[5]

Although the lattice parameters were different from each other beyond the experimental error (esd) in all the single crystals of **1**, tight-binding calculation based on the observed structures gave practically identical band structures and Fermi surfaces to each other (Table S5, ESI†). However, closer comparison of overlap integrals revealed a trend that transfer integrals I, III, and IV (Table S5, ESI†) are greater for insulating crystals than those for superconducting crystals. Similarly, the transfer integral II is greater for superconducting crystals than those for insulating crystals. These features may explain the qualitative differences in the observed conducting properties. Typical patterns of electrical behaviour with increasing R (%) (for R, see below) is shown in Fig. 2, exhibiting superconducting (SC), insulating (Ins), and intermediate (IM) behaviour among them. The IM behaviour should originate from a mixed phase of SC and Ins domains as discussed below. The SC behaviour was characterized by a sudden decrease in resistivity at T_C and large positive magnetoresistance below T_C. The Ins behaviour was characterized by a substantial increase in resistivity after decreasing the temperature to 2 K, in addition to negligible magnetoresistance. Thus, differences in the electrical behaviour under magnetic fields distinguish between superconductors and insulators. The application of magnetic fields indicated that samples #1 and #3 were insulators whereas sample #5 was a superconductor. An Arrhenius plot of the electrical behaviour of #1–#4 (Fig. S2, ESI†) evidently shows that they are not band insulators. Rather, all samples examined in this work exhibit a nearly temperature-independent electrical behaviour above ~80 K (Fig. 2), indicating a shared metallic band structure governed by the characteristic ET arrangement that forms conduction sheets called κ-type (Fig. 1). Thus **1** crossovers from a metallic to an insulating/superconducting phase or to intermediate behaviour at some lower temperature than 80 K. Furthermore, most samples with SC or IM behaviour exhibited an anomaly at T^* ≈ 8 K (Fig. S3, ESI†), below which a large magnetoresistance was commonly observed in the SC and IM samples (Fig. 2). The energy scale of T^* is significantly lower than the energy difference between the two conformations (0.81 eV ~ 9400 K) and was shifted to lower temperatures under an applied magnetic field (Fig. 2(d)).[6] Based on these

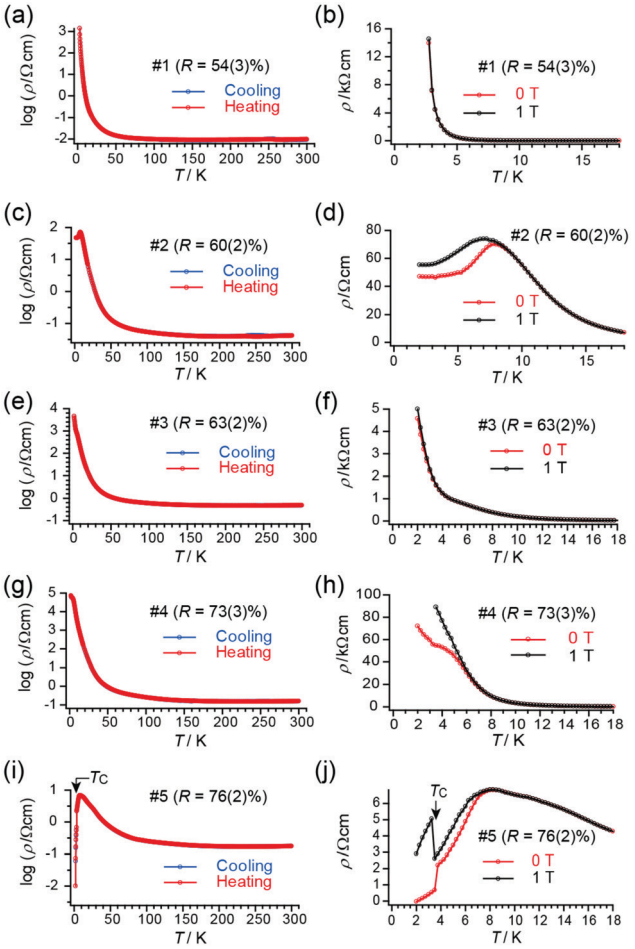

Fig. 2 Three types of electrical behaviour of **1** were monitored by a direct-current four-probe method using single crystals: superconducting (SC), insulating (Ins), and intermediate (IM) behaviour between SC and Ins. (a), (c), (e), (g), and (i) overall behaviour (2–300 K) without magnetic fields. (b), (d), (f), (h), and (j) the effect of the magnetic field (1 T) during the heating (2 → 18 K) processes by independent measurements using the same crystals (#1–#5) as those in (a), (c), (e), (g), and (i) for (b), (d), (f), (h), and (j), respectively. Some of the data collected under different conditions overlapped completely in the given scales of the plot. *R* (%) with the estimated standard deviation in parentheses denote the ratio of the staggered conformation in one of the ethylene groups in ET in each sample at 100 K under the slow (−1 K min^{-1}) cooling condition.

observations, we consider that T^* corresponds to the onset of a higher-T_c SC transition, whereas the SC domains are still minor parts which have not developed to form a continuous conduction pathway through the crystal. In fact, some crystals exhibited SC transitions at $T_c \sim T^* \sim 8$ K (Fig. S4, ESI†). Regardless of whether the SC behaviour was obvious or not, the volume fraction of the SC domains in **1** was often small based on the observed high residual resistivity (Fig. 2(d)), temperature-dependent resistivity below T^* (∼ 8 K) (Fig. 2(h)), and limited decrease in resistivity at T_c (Fig. 2(j)). The small fraction and rather low T_c (∼4 K) often observed for **1** as crystal-dependency observed in this work as well as in previous work[5j] are consistent with disorder in the ethylene groups, which hinder the coherence from developing in the entire crystal between the wave function of Cooper pairs during the SC transition. Samples #2 and #4 show IM behaviour of a superconductor (#5) and insulator (#1 and #3), exhibiting both SC-like large positive magnetoresistance and Ins-like high resistivity below 8 K. The substantial increase in resistivity at $T < \sim 80$ K is similar between the Ins (#1 and #3) and IM (#4) samples, in sharp contrast with the resistivity behaviour of the SC (#5) and other IM (#2) samples.

Next, we address the connection between the observed electrical behaviour and the crystal structure. The X-ray structure analyses revealed that all the examined single crystals contained disorder in one of the two ethylene groups on each ET molecule (Fig. 3), without evidence of defects or disorder in the polymer anions. The ET molecules in **1** are classified as eclipsed (*E*) and staggered (*S*) conformations.[5] We discuss the ratio between the two conformations *R* at a given temperature *T*,

$$R(T) = S/(S + E)$$

where *S* and *E* describe the number of staggered and eclipsed ethylene conformations in the disordered ethylene groups, respectively. Depending on the conditions of electrocrystallisation, including slight differences in the amount of crown ether or shape of the electrolytic cells, *R* differed from crystal to crystal in **1**, varying up to a few percent between crystals in the same batch. We were unable to control *R* during synthesis by electrocrystallisation conditions. All disordered ethylene groups were bonded to the iodine atoms *via* hydrogen bonds (Tables S3 and S4, ESI†). The hydrogen bonds C–H–X and disordered ethylene groups affecting conducting properties are commonly observed in κ-$ET_2Cu[N(CN)_2]X$ (X = Cl, Br, and I).[5] However, such structural features vary in **1** depending on the sample preparation conditions mentioned above. Differences in electrical behaviour among different crystals were seldomly observed at $T \geq 80$ K. Regardless of whether the disorder was static or dynamic, the ethylene groups vibrate intensely at higher temperatures, which averages the random potential originating from the disorder and makes the electrical

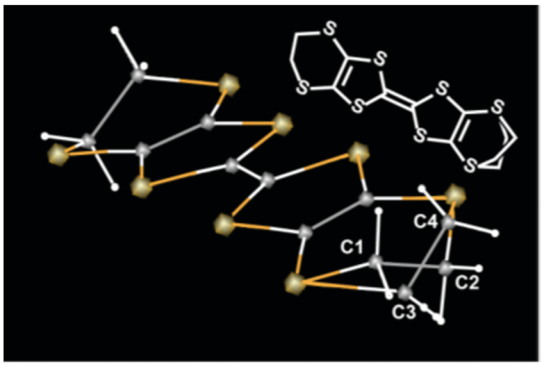

Fig. 3 Two conformations of the disordered ethylene group of ET in **1**. C1–C2: staggered and C3–C4: eclipsed forms. The hydrogen bond lengths at 100 K are (staggered) C–H···I: 3.286 and (eclipsed) C–H···I: 3.223 Å (Sample #2; *R* = 60(2)% at 100 K when cooled with −1 K min^{-1}). Hydrogen atoms were located based on the Fourier maps and were refined using the riding model.

behaviour common to different crystals. This interpretation is consistent with the nearly temperature-independent and low electrical resistivity observed at ~80–300 K as well as previous studies.[5m,n] In contrast, differences in R differed in electrical behaviour at $T \leq 80$ K (Fig. 2). Glass transitions originating from the ethylene-group disorder was observed at ~80 K in κ-$ET_2Cu[N(CN)_2]X$ (X = Cl, Br, and I).[5b–e,g,h,m] We examined different cooling processes by combining cooling rates (1 and 10 K min^{-1}) and temperatures where the cooling rate was changed (100, 40, 18, and 15 K) (For details, see ESI†). Although none of the observed electrical behaviour (Fig. 2) exhibited obvious anomalies associated with the glass transition, the electrical behaviour differed in qualitative or quantitative temperature-dependences depending on the values of R. The observed sensitive dependence of the electrical behaviour on the details of cooling processes below 80 K suggests significant effects of the glass transition on the ground states of **1**. In addition, spin fluctuations may also affect the electrical behaviour at $T \leq 80$ K.[7] In fact, negative magnetoresistance was observed around incomplete or broad SC transitions in some crystals of **1**. For example, the resistivity suddenly decreased around T_C (~8–9 K) under an applied magnetic field as shown in Fig. S4(b) (ESI†). Negative magnetoresistance is usually observed in magnetic metallic systems and is unusual for non-magnetic metallic systems such as **1**. Below 80 K, the spin fluctuation appeared in the crystal with R(100 K) ~70% (Fig. S4, ESI†). The value of R depended on the temperature but was independent of the cooling rates at $T \geq 100$ K (Table S2, ESI†). The details of the cooling processes down to ~20 K often qualitatively affected the electrical behaviour of **1**, and since the ethylene conformation should almost freeze at $T \leq 80$ K, the electronic (*i.e.*, charge and spin) degrees of freedom explicitly affect the electrical behaviour at $T \leq 80$ K. As a result, the electrical behaviour was more complicated at $T \leq 80$ K, depending on the details of the cooling processes. The relationship between R and various cooling processes at $T \leq 80$ K is currently under investigation. Recently, we observed a single crystal of **1** consisting of SC and Ins domains using time-and space-resolved spectroscopy.[8] It was not successful to try to transform Ins crystals into SC crystals, or *vice versa*, simply by changing the cooling processes. Accordingly, the ethylene conformation, and thus the values of R, may not vary drastically at $T < 80$ K. Therefore, in addition to the effect of the electronic degrees of freedom at $T < 80$ K, the values of R with which the crystals were produced during the electrocrystallisation are important factor for the conduction properties. By comparing the observed electrical behaviour of the single crystals with varied R under different cooling conditions, it has been found that R(100 K; under −1 K min^{-1}) more than ~73–75% should be the requirement for **1** to exhibit a superconducting transitions at 4–8 K with zero-resistance in the ground states (Fig. 4). The value of R = 75% is commensurate with the 3/4-filled band of **1**, which could favour a Mott Ins state because of the effectively 1/2-filled band. Meanwhile, the higher values of R than 75% are commensurate with none of $c^*/2$, $c^*/3$, and $0.38c^*$ superstructures, all of which have been reported to favour the Ins states.[5g,j,k,n] In this way, R could be associated with Coulomb interactions and electronic correlations. In actual crystals, the disorder, *i.e.*, inhomogeneous distribution of E and S conformations would favour the formation of Ins or SC domains which differ in R between themselves. The larger ionic radius and lower electronegativity of iodine atoms than other halogen atoms produce characteristically weak hydrogen bonds I···H–C(ethylene), which, in turn, produce various states with similar stabilities including metastable SC and Ins states.

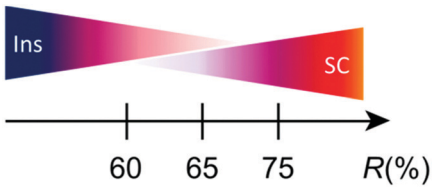

Fig. 4 Relationship between the ground states and ratio (R%) of staggered conformation in the disordered ethylene groups at 100 K in **1** (cooling rate: −1 K min^{-1}). The observed behaviour is intermediate between superconducting (SC) and insulating (Ins) properties in the range $R \approx 60$–73% in that the behaviour exhibits both characteristic of SC (large positive magnetoresistance below a certain temperature) and that of Ins (increasing resistivity toward 2 K). Note that the ground state is also highly sensitive to the details of cooling processes, and that R is not an only parameter to determine the ground states. The figure describes an approximate trend.

The factors such as charge and spin degrees of freedom, bandwidth, Coulomb interactions, and overlap integrals between the HOMOs of ET have been paid attention to explain the observed various types of electrical behavior of the κ-type superconductors.[5] However, our findings have revealed that R is also one of the important factors to determine the electrical behaviour and the ground state of **1**. Although both effects of ethylene disorder and ethylene conformation on the superconductivity of organic conductors have been known for a long time from various points of view including related κ-OCTCs,[5] **1** is unique in that the ethylene conformation sensitively changes in a wide range depending on the details of crystallization conditions and cooling processes. This structural feature makes the electrical behaviour at $T \leq 80$ K depend on both R and details of cooling processes at $T \leq 80$ K, which in turn makes the behaviour complicated and non-systematic in terms of R or the phase diagrams.

In summary, R is sensitively dependent on temperature and synthetic conditions, and is an important factor to determine the ground states to be SC or Ins properties. The values of R affect on the band structure *via* superstructures, and can be associated with electronic interactions *via* electron–phonon interactions in **1**. Yet, the weak hydrogen bonds I···H–C(ethylene) cause disorder in the ethylene conformations, which in turn cause complicated electrical and structural behaviours, being sensitive to cooling processes, and producing the unique dynamics and the exceptional position of **1** in the universal κ-OCTC diagrams.

Conclusions

We found that the ground state and electrical properties of **1** are affected by the ratio of two kinds of ethylene conformations,

which vary from crystal to crystal and are affected by sample preparation. Accordingly, the electrical behaviour cannot be explained by the universal phase diagrams proposed for κ-OCTCs;[3] furthermore, inconsistent and/or irreproducible electrical behaviours have previously been observed among different research groups and crystals. Since there remains unsolved problems regarding the structure-conduction correlation in κ-OCTCs,[9] our findings shed light on the controversial situation regarding the electrical behaviour and superconducting mechanism of κ-OCTCs. Because superconducting mechanism should be largely based on electron–phonon interactions, the active role of a molecular vibration revealed in this work is an important step forward to the future control of the conduction electrons in molecular crystals exhibiting considerably high T_Cs.

Conflicts of interest

There are no conflicts to declare.

Acknowledgements

The assistance of S. Mori and R. Konishi (Ehime University) for X-ray structural analyses is acknowledged. The authors thank K. Konishi (Ehime University) for access to the PPMS (Quantum Design PPMS-9). This work was partially supported by Grant-in-Aid for Challenging Exploratory Research (18K19061) and Grant-in-Aid for Scientific Research (C) (15K05478, 19K05405) of JSPS, the Tokyo Chemical Industry Foundation, the Tokyo Ohka Foundation for the Promotion of Science and Technology, the Kato Foundation for Promotion of Science, the Iketani Science and Technology Foundation (ISTF; 0331005-A), Casio Science Promotion Foundation, and an Ehime University Grant for Project for the Promotion of Industry/University Cooperation.

Notes and references

1 (*a*) R. Murase, B. Ding, Q. Gu and D. M. D'Alessandro, *Philos. Trans. R. Soc., A*, 2019, **377**, 20180226; (*b*) J.-P. Pouget, P. Alemany and E. Canadell, *Mater. Horiz.*, 2018, **5**, 590; (*c*) H. Jiang, P. Hu, J. Ye, K. K. Zhang, Y. Long, W. Hu and C. Kloc, *J. Mater. Chem. C*, 2018, **6**, 1884; (*d*) F. Kagawa and H. Oike, *Adv. Mater.*, 2017, **29**, 1601979; (*e*) B. Náfrádi, M. Choucair and L. Forró, *Adv. Funct. Mater.*, 2017, **27**, 1604040; (*f*) S. E. Brown, *Phys. C*, 2015, **514**, 279; (*g*) P. Monceau, *Adv. Phys.*, 2012, **61**, 325.

2 (*a*) S. Fukuoka, S. Fukuchi, H. Akutsu, A. Kawamoto and Y. Nakazawa, *Crystals*, 2019, **9**, 66; (*b*) J. Wosnitza, *J. Low Temp. Phys.*, 2007, **146**, 641; (*c*) B. J. Powell and R. H. McKenzie, *J. Phys.: Condens. Matter*, 2006, **18**, R827; (*d*) K. Miyagawa, K. Kanoda and A. Kawamoto, *Chem. Rev.*, 2004, **104**, 5635.

3 (*a*) T. Sasaki, *Crystals*, 2012, **2**, 374; (*b*) T. Sasaki, Infrared imaging in the strongly correlated molecular conductors in Molecular Electronic and Related Materials–Control and Probe with Light, ed. T. Naito, Transworld Research Network, Kerala, India, 2010, ch. 4, pp. 99–116; (*c*) D. Faltermeier, J. Barz, M. Dumm, M. Dressel, N. Drichko, B. Petrov, V. Semkin, R. Vlasova, C. Mézière and P. Batail, *Phys. Rev. B: Condens. Matter Mater. Phys.*, 2007, **76**, 165113; (*d*) K. Kanoda, *J. Phys. Soc. Jpn.*, 2006, **75**, 051007; (*e*) T. Sasaki, I. Ito, N. Yoneyama, N. Kobayashi, N. Hanasaki, H. Tajima, T. Ito and Y. Iwasa, *Phys. Rev. B: Condens. Matter Mater. Phys.*, 2004, **69**, 064508; (*f*) P. Limelette, P. Wzietek, S. Florens, A. Georges, T. A. Costi, C. Pasquier, D. Jérome, C. Mézière and P. Batail, *Phys. Rev. Lett.*, 2003, **91**, 016401; (*g*) D. Fournier, M. Poirier, M. Castonguay and K. Truong, *Phys. Rev. Lett.*, 2003, **90**, 127002; (*h*) T. Sasaki, N. Yoneyama, A. Matsuyama and N. Kobayashi, *Phys. Rev. B: Condens. Matter Mater. Phys.*, 2002, **65**, 060505(R); (*i*) J. Müller, M. Lang, F. Steglich, J. A. Schlueter, A. M. Kini and T. Sasaki, *Phys. Rev. B: Condens. Matter Mater. Phys.*, 2002, **65**, 144521; (*j*) S. Lefebvre, P. Wzietek, S. Brown, C. Bourbonnais, D. Jérome, C. Mézière, M. Fourmigué and P. Batail, *Phys. Rev. Lett.*, 2000, **85**, 5420; (*k*) K. Kanoda, *Hyperfine Interact.*, 1997, **104**, 235; (*l*) H. Ito, T. Ishiguro, M. Kubota and G. Saito, *J. Phys. Soc. Jpn.*, 1996, **65**, 2987; (*m*) H. Kino and H. Fukuyama, *J. Phys. Soc. Jpn.*, 1996, **65**, 2158.

4 (*a*) R. T. Clay and S. Mazumdar, *Phys. Rep.*, 2019, **788**, 1; (*b*) R. A. Klemm, *Phys. C*, 2015, **514**, 86; (*c*) S. Mazumdar and R. T. Clay, *Int. J. Quant. Chem.*, 2014, **114**, 1053; (*d*) M. R. Norman, *Science*, 2011, **332**, 196; (*e*) E. Demler, W. Hanke and S.-C. Zhang, *Rev. Mod. Phys.*, 2004, **76**, 909; (*f*) Y. Yanase, T. Jujo, T. Nomura, H. Ikeda, T. Hotta and K. Yamada, *Phys. Rep.*, 2003, **387**, 1; (*g*) R. H. McKenzie, *Science*, 1997, **278**, 820; (*h*) H. Fukuyama and Y. Hasegawa, *Physica B + C*, 1987, **148**, 204.

5 (*a*) T. Kobayashi, A. Suzuta, K. Tsuji, Y. Ihara and A. Kawamoto, *Phys. Rev. B: Condens. Matter Mater. Phys.*, 2019, **100**, 195115; (*b*) A. U. B. Wolter, R. Feyerherm, E. Dudzik, S. Süllow, Ch Strack, M. Lang and D. Schweitzer, *Phys. Rev. B: Condens. Matter Mater. Phys.*, 2007, **75**, 104512; (*c*) C. Strack, C. Akinci, V. Pashchenko, B. Wolf, E. Uhrig, W. Assmus, M. Lang, J. Schreuer, L. Wiehl, J. A. Schlueter, J. Wosnitza, D. Schweitzer, J. Müller and J. Wykhoff, *Phys. Rev. B: Condens. Matter Mater. Phys.*, 2005, **72**, 054511; (*d*) M. Maksimuk, K. Yakushi, H. Taniguchi, K. Kanoda and A. Kawamoto, *Synth. Met.*, 2005, **149**, 13; (*e*) N. Yoneyama, T. Sasaki, T. Nishizaki and N. Kobayashi, *J. Phys. Soc. Jpn.*, 2004, **73**, 184; (*f*) H. Taniguchi, K. Kanoda and A. Kawamoto, *Phys. Rev. B: Condens. Matter Mater. Phys.*, 2003, **67**, 014510; (*g*) V. S. Yefanov, S. Kagoshima, R. Kondo, M. A. Tanatar, N. D. Kushch and E. B. Yagubskii, *Synth. Met.*, 2003, **137**, 1295; (*h*) M. Pinterić, S. Tomić, M. Prester, Đ. Drobac and K. Maki, *Phys. Rev. B: Condens. Matter Mater. Phys.*, 2002, **66**, 174521; (*i*) J. Müller, M. Lang, F. Steglich, J. A. Schlueter, A. M. Kini and T. Sasaki, *Phys. Rev. B: Condens. Matter Mater. Phys.*, 2002, **65**, 144521; (*j*) M. A. Tanatar, T. Ishiguro, S. Kagoshima, N. D. Kushch and E. B. Yagubskii, *Phys. Rev. B: Condens. Matter Mater. Phys.*, 2002, **65**, 064516; (*k*) N. D. Kushch, M. A. Tanatar, T. Ishiguro, S. Kagoshima,

E. B. Yagubskii, V. S. Yefanov and V. A. Bondarenko, *Synth. Met.*, 2003, **133–134**, 177; (*l*) V. S. Yefanov, M. A. Tanatar, T. Ishiguro, H. Ito, V. A. Bondarenko, N. D. Kushch and E. B. Yagubskii, *Synth. Met.*, 2001, **120**, 959; (*m*) N. D. Kushch, M. A. Tanatar, E. B. Yagubskii and T. Ishigur, *JETP Lett.*, 2001, **73**, 429; (*n*) M. A. Tanatar, S. Kagoshima, T. Ishiguro, H. Ito, V. S. Yefanov, V. A. Bondarenko, N. D. Kushch and E. B. Yagubskii, *Phys. Rev. B: Condens. Matter Mater. Phys.*, 2000, **62**, 15561; (*o*) H. Akutsu, K. Saito and M. Sorai, *Phys. Rev. B: Condens. Matter Mater. Phys.*, 2000, **61**, 4346; (*p*) M. A. Tanatar, T. Ishiguro, T. Kondo and G. Saito, *Phys. Rev. B: Condens. Matter Mater. Phys.*, 1999, **59**, 3841; (*q*) K. Andres, *Synth. Met.*, 1998, **94**, 11; (*r*) M. Kund, H. Müller, N. D. Kushch, K. Andres and G. Saito, *Synth. Met.*, 1995, **70**, 951; (*s*) T. Burgin, T. Miebach, J. C. Huffman, L. K. Montgomery, J. A. Paradis, C. Rovira, M.-H. Whangbo, S. N. Magonov, S. I. Khan, C. E. Strouse, D. L. Overmyer and J. E. Schirber, *J. Mater. Chem.*, 1995, **5**, 1659; (*t*) V. Kataev, G. Winkel, D. Khomskii, D. Wohlleben, W. Crump, K. F. Tebbe and J. Hahn, *Solid State Commun.*, 1992, **83**, 435; (*u*) H. H. Wang, K. D. Carlson, U. Geiser, A. M. Kini, A. J. Schultz, J. M. Williams, L. K. Montgomery, W. K. Kwok, U. Welp, K. G. Vandervoort, S. J. Boryschuk, A. V. Strieby Crouch, J. M. Kommers, D. M. Watkins, J. E. Schirber, D. L. Overmyer, D. Jung, J. J. Novoa and M.-H. Whangbo, *Synth. Met.*, 1991, **41–43**, 1983; (*v*) J. M. Williams, A. J. Schultz, U. Geiser, K. D. Carlson, A. M. Kini, H. H. Wang, W.-K. Kwok, M.-H. Whangbo and J. E. Schirber, *Science*, 1991, **252**, 1501; (*w*) D. Jung, M. Evain, J. J. Novoa, M.-H. Whangbo, M. A. Beno, A. M. Kini, A. J. Schultz, J. M. Williams and P. J. Nigrey, *Inorg. Chem.*, 1989, **28**, 4516; (*x*) J. M. Williams, M. A. Beno, H. H. Wang, P. C. W. Leung, T. J. Emge, U. Geiser and K. D. Carlson, *Acc. Chem. Res.*, 1985, **18**, 261.

6 For details of calculation, see ESI†.

7 (*a*) A. Kawamoto, K. Miyagawa, Y. Nakazawa and K. Kanoda, *Phys. Rev. Lett.*, 1995, **74**, 3455; (*b*) A. Kawamoto, K. Miyagawa, Y. Nakazawa and K. Kanoda, *Phys. Rev. B: Condens. Matter Mater. Phys.*, 1995, **52**, 15522.

8 S. Tsuchiya, R. Kuwae, T. Kodama, Y. Nakamura, M. Kurihara, T. Yamamoto, T. Naito and Y. Toda, *J. Phys. Soc. Jpn.*, 2020, **89**, 064712.

9 T. Kawamoto, T. Mori, A. Nakao, Y. Murakami and J. A. Schlueter, *J. Phys. Soc. Jpn.*, 2012, **81**, 023705.